

ARTICLE IN PRESS – Acta Cryst. E

CRYSTALLOGRAPHIC
COMMUNICATIONS

ISSN 2056-9890

Bis(catecholato- κ^2O,O')bis(dimethyl sulfoxide- κO)titanium(IV)**Proof instructions**

Proof corrections should be returned by **13 March 2022**. After this period, the Editors reserve the right to publish your article with only the Managing Editor's corrections.

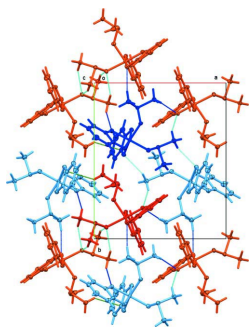
Please

- (1) Read these proofs and assess whether any corrections are necessary.
- (2) Check that any technical editing queries highlighted in **bold underlined** text have been answered.
- (3) Send corrections by e-mail to **checkin@iucr.org**. Please describe corrections using plain text, where possible, giving the line numbers indicated in the proof. Please do not make corrections to the pdf file electronically and please do not return the pdf file. If no corrections are required please let us know.

If you wish to purchase printed offprints, please complete the attached order form and return it by e-mail as soon as possible.

Please check the following details for your article

Abbreviated author list: Hewage, N.; Mastriano, C.; Brückner, C.; Zeller, M.



Thumbnail image for contents
page

How to cite your article in press

Your article has not yet been assigned page numbers, but may be cited using the doi:

Hewage, N., Mastriano, C., Brückner, C. & Zeller, M. (2022). *Acta Cryst.* **E78**, <https://doi.org/>.

You will be sent the full citation when your article is published and also given instructions on how to download an electronic reprint of your article.



Received 23 February 2022

Accepted 8 March 2022

Edited by J. Reibenspies, Texas A & M University, USA

Keywords: transition-metal catecholates; heteroleptic catecholates; titanium catecholates; crystal structure.

CCDC reference: 2157170

Supporting information: this article has supporting information at journals.iucr.org/e

Bis(catecholato- κ^2O,O')bis(dimethyl sulfoxide- κO)titanium(IV)

Nisansala Hewage,^a Carolyn Mastriano,^a Christian Brückner^{a*} and Matthias Zeller^b

^aDepartment of Chemistry, University of Connecticut, Storrs, CT 06269-3060, USA, and ^bDepartment of Chemistry, Purdue University, 560 Oval Drive, West Lafayette, IN, 47907-2084, USA. *Correspondence e-mail: c.bruckner@uconn.edu

Bis(benzene-1,2-diolato- κ^2O,O')bis(dimethyl sulfoxide- κO)titanium(IV), [Ti(C₆H₄O₂)₂(C₂H₆OS)₂], crystallizes with two crystallographically independent molecules in the space group $P2_1/c$ emulating orthorhombic $Pbca$ symmetry ($\beta = 90.0445(9)^\circ$). The two molecules are related by pseudo-glide symmetry, broken by modulation of each one catecholate and dimethyl sulfoxide (DMSO) ligand. Twinning by pseudomerohedry was observed [twin ratio 0.5499 (7):0.4401 (7)]. Complex **3** was obtained by heating of diprotonated titanium tris-catecholate precursor **2^H** in DMSO, by formal displacement of a catechol molecule by two DMSO molecules. Complex **3** is just the second heteroleptic, mono-nuclear, neutral bis-catecholate complex with TiO₆ metal coordination, the only other one being its bis-DMF analogue **6**. The two molecules of **3** exhibit a distorted octahedral geometry. The geometry and distortions from ideal symmetry of **3** are discussed and compared to **6** and to cationic tris-catecholate titanium complexes.

1. Chemical context

The dianion of catechol (1,2-dihydroxybenzene, CatH, **1**) is a bidentate, dianionic and non-innocent *O,O*-chelating agent with a particularly high affinity for HSAB hard-metal ions, *i.e.*, ions of high oxidation states or high charge-to-metal-ion-radius ratios (Pierpont & Lange, 1994; Kaim & Schwederski, 2010). Titanium(IV) is one such metal ion and long known to form stable, pseudooctahedral triscatecholate complexes, such as **2^{Et3NH}**, by reaction of catechol with Ti⁴⁺ sources under basic conditions (Fig. 1) (Borgias *et al.*, 1984).

Titanium catecholate complexes have found various uses: Titanium triscatecholate complexes of the alkaline earth metals were utilized as molecular precursors to a number of

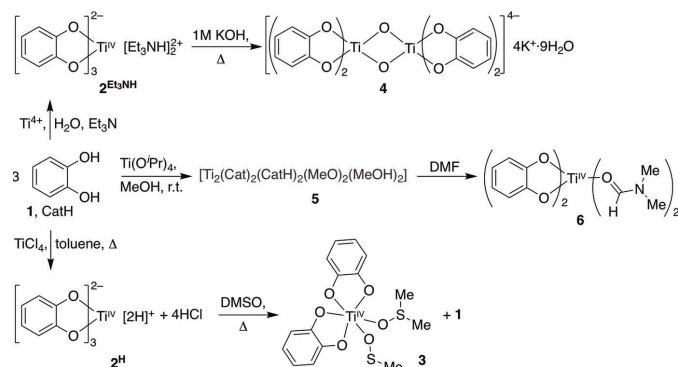
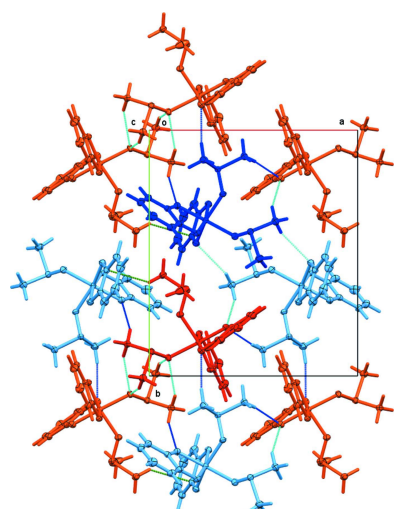


Figure 1
Formation of titanium(IV) catecholate complexes, including the title compound **3**.



Published under a CC BY 4.0 licence

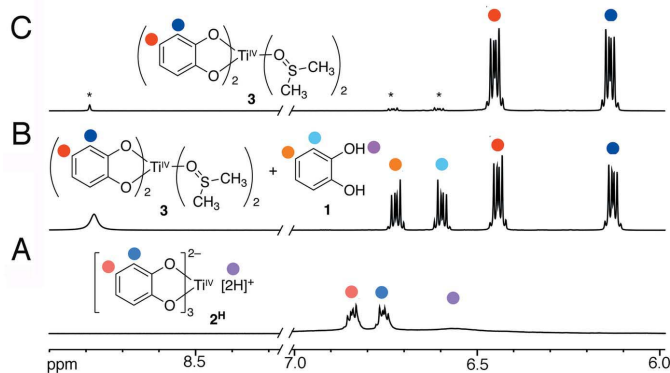


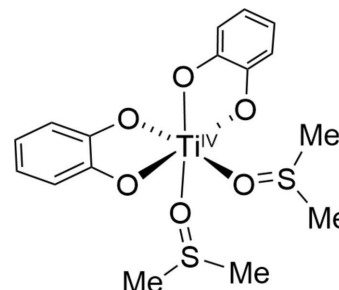
Figure 2
 ^1H NMR spectra (400 MHz, $\text{DMSO}-d_6$) of (A) complex 2^{H} dissolved at ambient temperature; (B) of complex 2^{H} at ~ 373 K, showing the presence of complex **3** and free catechol **1**; (C) of isolated crystals of **3** precipitated from DMSO at ambient temperature (* indicates the presence of residual **1**).

$\text{M}^{\text{II}}\text{TiO}_6$ -type perovskites (Ali & Milne, 1987; Marteel-Parrish *et al.*, 2008). Titanium catecholates have been exploited as catalysts in acetylene hydrogenation (Bazhenova *et al.*, 2016) while three-dimensional titanium catecholate frameworks of high proton conductivity (Nguyen *et al.*, 2015) and titanium catecholate-based MOFs have been described (Cao *et al.*, 2020). Metal catecholates have been suggested as adsorbents for toxic gases (Bobbitt & Snurr, 2018). Titanium tris-catecholates were also used to self-assemble a potential bimodal contrast agent (Dehaen *et al.*, 2012). A number of heteroleptic mono- and multi-nuclear titanium complexes do contain titanium catechol units (Sakata *et al.*, 2010; Bazhenova *et al.*, 2016; Sonström *et al.*, 2019; Passadis *et al.*, 2020) (for further examples, see *Database survey* below). Most prominently, titanium tris-catecholates have been used as versatile building blocks in a range of supramolecular, oligonuclear homo- and hetero-metal-ligand cluster assemblies (Brückner *et al.*, 1998; Caulder *et al.*, 2001; Albrecht *et al.*, 2008, 2019).

Reaction of TiCl_4 under anhydrous conditions in toluene generates a brick-colored amorphous powder of the diprotonated titanium tris-catecholate complex 2^{H} (Davies & Dutremez, 1990). We found that this compound dissolves sufficiently enough in ambient-temperature $\text{DMSO}-d_6$ to record a simple ^1H NMR spectrum, showing only two multiplets of equal integration (at 6.84 and 6.75 ppm), corresponding to the *ortho*- and *meta*-hydrogens on three near-identical catecholate moieties (the counter-cations – protons – are believed to be dynamically associated with the trigonal faces of the pseudo-octahedral coordination sphere formed by the six catecholate oxygens) (Fig. 2A). Upon heating 2^{H} in DMSO (or $\text{DMSO}-d_6$), its solubility increases drastically. When followed by ^1H NMR spectroscopy, the formation of a new species with two catecholate signals (*m* at 6.42 and 6.12 ppm, in 2:2 intensity) and 1 equivalent of free catechol (*m* at 6.73 and 6.60, *br s* at 8.1 ppm, all 1:1:1) can be observed (Fig. 2B). Upon cooling, dark red–orange crystals of the title compound **3** formed. Isolated and analyzed by NMR spectroscopy, they exhibit only the signals for the new species

formed (Fig. 2C) and the signals for ~~some~~ two slightly high-field-shifted DMSO molecules (not shown).

The material was also analyzed by single crystal X-ray diffraction (Fig. 3). Evidently, one protonated catecholate ligand (*i.e.*, catechol **1**) of the starting triscatecholate complex 2^{H} was exchanged for two DMSO molecules, coordinating through their oxygen atoms in adjacent positions, thus forming a neutral, heteroleptic, mononuclear octahedral complex. Details of the structural arrangement will be discussed in the *Structural commentary* section below.



3

The UV–vis spectrum of the orange solution of **3** is overall similar to that of the starting material 2^{H} ; both spectra are dominated in the visible range by broad, little-structured catecholate ligand-to-metal charge-transfer bands (for **3**, $I_{\text{max}} = 441$ nm; half-height width > 150 nm; Fig. 4). In comparison to the spectrum of 2^{H} , all bands for **3** are bathochromically shifted.

2. Structural commentary

The title complex **3**, having solution C_2 symmetry, crystallizes as a racemic mixture with two crystallographically independent molecules in the monoclinic space group $P2_1/c$ (Fig. 3).

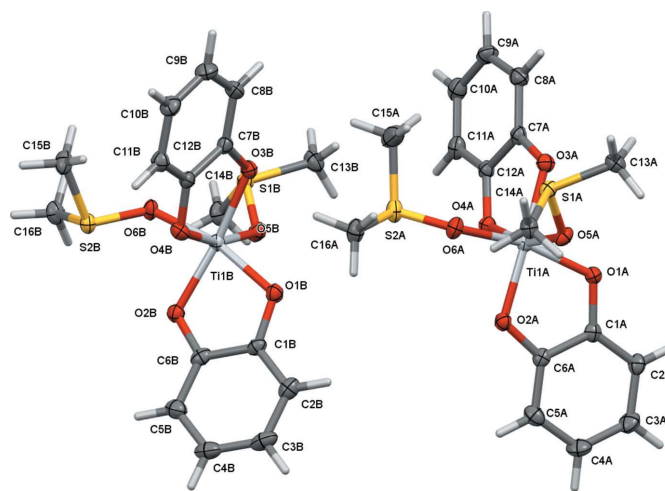


Figure 3
 The two crystallographically independent molecules of **3**. View along the *a* axis. Molecules *A* and *B* are related by pseudo-glide operations (see discussion for details).

Table 1

Continuous shape measures (CShM's) relative to ideal reference octahedral symmetry for $2^{\text{Et}_3\text{NH}}$, **3** and **6**.

Structure	Hexagon	Pentagonal pyramid	Octahedron	Trigonal prism	Johnson pentagonal pyramid J2
$2^{\text{Et}_3\text{NH}}$	33.773	23.482	1.434	9.808	27.215
3A	32.792	22.191	1.491	10.655	26.183
3B	32.830	21.007	1.854	10.159	24.952
6	33.664	22.467	1.513	10.069	26.511

For both molecules, the solution C_2 symmetry is broken in the solid state, and the Ti atoms are each bonded to two chelating catecholate and two monodentate O-coordinated dimethylsulfoxide ligands. The Ti—O_{Cat} bond distances range from 1.9113 (19) to 1.9564 (18) Å in molecule *A*, and 1.9108 (18) to 1.9545 (18) in molecule *B* [average 1.93 (3) Å]. A notable structural *trans*-effect is observed as the longer distances are observed for the oxygen atoms opposite another catechol oxygen donor atom [1.9346 (18) to 1.9564 (18) Å] while the shorter distances [1.9108 (18) to 1.9284 (19) Å] are found *trans* to the weaker electron-donating O_{DMSO} atoms.

The Ti—O_{Cat} bond distances in the cationic triscatecholate complex $2^{\text{Et}_3\text{NH}}$ are on average longer [1.97 (3) vs 1.93 (3) Å in **3**], ranging from 1.941 (1) to 2.014 (1) Å with differences between long and short Ti—O bonds caused by distortion from strong hydrogen bonds to the Et₃NH⁺ counter-cations (reflected in a 0.05 Å lengthening of the associated Ti—O bonds) (Borgias *et al.*, 1984). The four Ti—O_{DMSO} bond distances in **3** are at 2.0214 (19) to 2.0416 (18) Å significantly longer than the Ti—O_{Cat} bond lengths, as would be expected for neutral and uncharged DMSO ligands.

The bond lengths in **3** also compare well with those of the [biscatecholate-bis-DMF]titanium complex **6**, the DMF analogue to the title compound (Bazhenova *et al.*, 2016) and the only other reported heteroleptic mono-nuclear and uncharged bis-catecholate titanium complex with MO₆ metal coordination (see *Database survey*). The Ti—O_{Cat} bond lengths in **6** are 1.9003 (12) and 1.9181 (12) Å for the oxygen atoms *trans* to the DMF molecules, 1.9408 (11) and 1.9483 (11) Å when *trans* to another O_{Cat} atom, and 2.0396 (12) and 2.0736 (12) Å for the Ti—O_{DMF} bond lengths. They thus closely mirror those found in **3**.

The small bite angles of the chelating catecholate anions induce substantial distortions from idealized octahedral

symmetry. The catecholate O—Ti—O angles in **3** are 80.73 (7) and 81.00 (8)° in molecule *A* and 80.85 (8) and 80.24 (8)° in molecule *B*, which are essentially indistinguishable from those in $2^{\text{Et}_3\text{NH}}$ [80.1 (1) to 80.6 (1)°] and **6** [O3 80.68 (5) and O2 80.97 (5)°]. The other *cis* angles in **3** cover a wide range from as small as 82.35 (7)° (for the O_{DMSO}—Ti—O_{DMSO} angle in molecule *A*) to as large as 105.30 (8)° (for one of the O_{Cat}—Ti—O_{DMSO} angles in molecule *B*). The latter rather obtuse large angle is unique in being nearly 4° wider than the next largest angle [its equivalent in molecule *A* is 101.66 (8)°]. The angles in $2^{\text{Et}_3\text{NH}}$ do not exceed 101.3°. The equivalent angles in the DMF analogue **6** are more evenly distributed than in either molecule of **3**, ranging from 82.53 (5) to 97.77 (5)°.

This more pronounced deviation from ideal octahedral symmetry for molecule *B* of **3** is also confirmed by a more holistic analysis, using a normalized root-mean-square deviation algorithm to calculate the distortion from octahedral symmetry as implemented in the program *SHAPE* (Pinsky & Avnir, 1998; Alvarez *et al.*, 2002; Casanova *et al.*, 2004). The calculated continuous shape measures (CShM's) relative to ideal reference octahedral symmetry are 1.434 for $2^{\text{Et}_3\text{NH}}$, 1.513 for **6**, 1.491 for less distorted molecule *A* of **3**, and 1.854 for molecule *B* (Table 1). Shape measures may be between 0 and 100 where zero represents a perfect fit for the selected shape, and CShM values of less than 1.0 are usually interpreted as only minor distortions from the reference shape. Values between 1 and 3 indicate substantial distortions, but the reference shape still provides a good stereochemical description (Cirera *et al.*, 2005). For the four cases analyzed here, the CShM's for the next best fit, trigonal prismatic, are all around 10 (Table 1). The geometries of **3**, **6** and $2^{\text{Et}_3\text{NH}}$ are thus best described as distorted octahedral, being far removed from fitting any other polygon.

The two independent molecules in compound **3** are related to each other by crystallographic pseudosymmetry. Complex **3** crystallized in a pseudo-orthorhombic setting with a refined β angle of 90.0445 (9)°, and emulates space group *Pbca* with additional *b*- and *a*-glide operations along the *a*- and *c*-axis directions. Exact translational symmetry is broken by modulation of one of the catecholate and one of the DMSO ligands, as discussed below. The metric pseudosymmetry allows for the possibility of twinning. Indeed, the crystal investigated was found to be pseudo-merohedrally twinned by symmetry elements of the emulated orthorhombic symmetry. Application of the twin transformation matrix 1 0 0, 0 −1 0, 0 0 −1 yielded close to equal twin components with a refined twin ratio of 0.5499 (7) to 0.4401 (7).

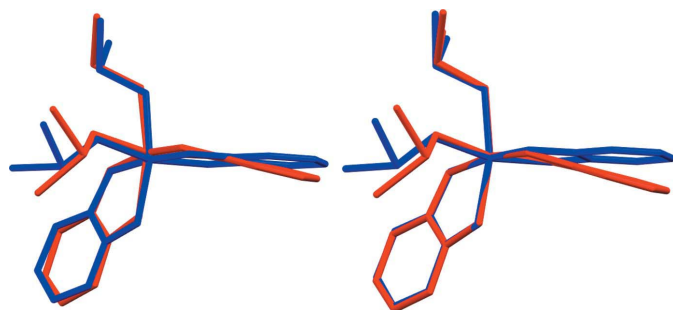


Figure 4

Normalized UV-vis spectrum of title compound **3** (DMSO) in comparison to that of the starting triscatecholate **1** (H₂O). **Please supply correct figure**

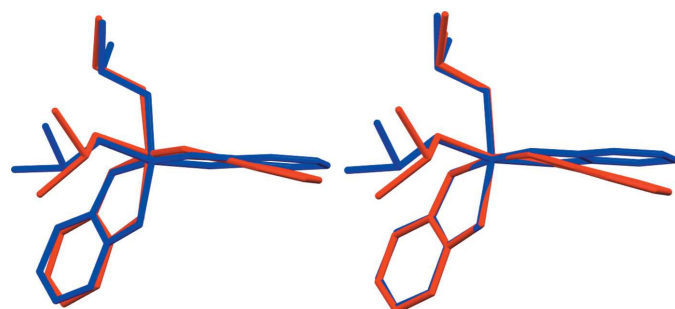


Figure 5

Root-mean-square overlays of the two independent molecules of **3**, after inversion of molecule *B* (red: molecule *A*; blue: molecule *B*). Left: fit based on all non-H atoms (r.m.s. deviation 0.459 Å). Right: fit based on Ti and O atoms only (r.m.s. deviation 0.056 Å).

A root-mean-square overlay of the two molecules yields an r.m.s. deviation of 0.459 Å, indicating substantial variation between the geometries of molecules *A* and *B* (Fig. 5). A similar overlay based on only the titanium and oxygen atoms gives a much smaller value of only 0.056 Å, indicating that the main differences between the two complexes is rooted in the ligands, even though there are small and noticeable differences for the TiO_6 cores as well (with molecule *B* deviating more from ideal octahedral symmetry than molecule *A*, as discussed above). The main distinction between the two molecules is, however, associated with substantial twists and torsions of the catecholate and DMSO ligands. The r.m.s.

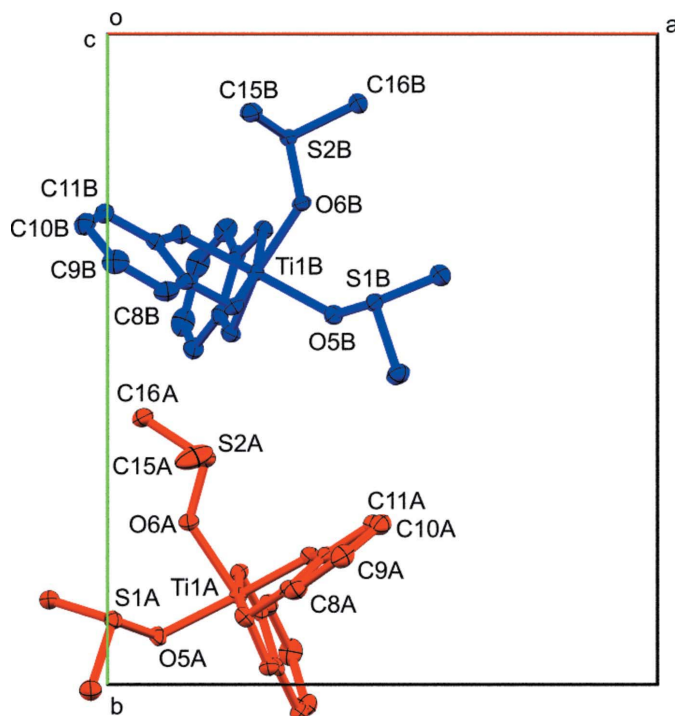


Figure 6

View of **3** down the *c* axis, showing the modulation by pseudo-*Pbca* symmetry. Molecules color coded by symmetry equivalence (red: molecule *A*, blue molecule *B*). Atom labels included for Ti, DMSO S and O atoms, and for C atoms with the largest modulation. 50% probability ellipsoids.

Table 2

Hydrogen-bond geometry (Å, °).

<i>D</i> —H··· <i>A</i>	<i>D</i> —H	H··· <i>A</i>	<i>D</i> ··· <i>A</i>	<i>D</i> —H··· <i>A</i>
C11A—H11A···O2B ⁱ	0.95	2.62	3.491 (3)	153
C13A—H13C···O5A ⁱⁱ	0.98	2.54	3.428 (3)	151
C14A—H14B···O1A ⁱⁱ	0.98	2.66	3.378 (3)	130
C14A—H14B···O5A ⁱⁱ	0.98	2.55	3.447 (3)	152
C14A—H14C···O4B ⁱⁱⁱ	0.98	2.27	3.193 (3)	156
C13B—H13E···O5B ⁱ	0.98	2.60	3.495 (4)	151
C14B—H14E···O4A ⁱ	0.98	2.55	3.438 (3)	151
C14B—H14F···O1B ⁱ	0.98	2.56	3.336 (3)	136
C15B—H15D···O3A ^{iv}	0.98	2.34	3.307 (3)	171
C16B—H16D···O1A ^{iv}	0.98	2.59	3.186 (3)	119
C16B—H16E···O4A ⁱ	0.98	2.45	3.427 (3)	173

Symmetry codes: (i) $-x+1, -y+1, -z+1$; (ii) $-x, -y+2, -z+1$; (iii) $-x, -y+1, -z+1$; (iv) $x, y-1, z$.

overlay reveals a close match of one of the catecholate ligands and one of the DMSO ligands. The other catecholate and DMSO ligands, on the other hand, do show substantial variation between the two molecules. The catecholate of C7–C12 undergoes a twist-motion by a slight rotation around the $\text{O}_{\text{cat}}-\text{O}_{\text{cat}}$ axis. In molecule *A* (blue in the overlay), the catecholate ligand is close to coplanar with the titanium atom, while in molecule *B* (red in the overlay) the catecholate and the $\text{TiO}(\text{Cat})_2$ plane are clearly angled against each other. The deviations of the Ti atoms from the mean catecholate planes are 0.049 (2) and 0.349 (2) Å for molecules *A* and *B*, respectively. The angle between the mean catecholate and $\text{Ti}(\text{OCat})_2$ planes is 1.97 (9)° for complex *A*, but a much larger value of 13.6 (8)° for complex *B*.

The other main difference between the two molecules is a rotation of about 14° for one of the two DMSO ligands around the Ti–O bond, which can be expressed *via* the torsion angle O5–Ti1–O6–S2 (S2 is the sulfur atom of the rotated DMSO ligand, O5 the oxygen atom of the other invariant DMSO ligand). These torsion angles are 165.13 (16)° for molecule *A*, and 151.10 (14)° for molecule *B*. The largest overall motion is observed for the DMSO methyl groups of C15 [1.774 (3) Å in the r.m.s. overlay based on the titanium and oxygen atoms].

The differences in molecular geometry between molecules *A* and *B* and the modulation by pseudo-orthorhombic symmetry are closely related, showing molecules *A* and *B* as they are related to each other by a pseudo *b*-glide perpendicular to (100) (Fig. 6). In addition to the variations in molecular geometry seen in the molecule overlay, a very slight rotation of the entire complex is also observed.

3. Supramolecular features

The most prominent directional interactions in complex **3** are medium strength C—H···O interactions, involving the DMSO methyl groups as hydrogen-bond donors, and catecholate and DMSO oxygen atoms as the respective acceptors. Hydrogen bonds with C···O distances below 3.50 Å are given in Table 2. Some of these H···O distances are unusually short for C—H···O interactions, with H···O distances as short as 2.27 and 2.34 Å, approaching distances usually only observed for clas-

sical hydrogen bonds involving acidic hydrogens. This might indicate stronger than usual interactions with a possibly larger influence on the packing and molecular arrangement in the solid state than usually observed for C—H...O interactions.

When plotting the C—H...O hydrogen bonds (Fig. 7), it becomes evident that the interactions are different for the two molecules, despite their close relationship by a pseudo-glide operation. Interactions involving the less modulated fragments of **3A** and **3B** exhibit similar hydrogen-bonding environments. C13 and C14 of the less-modulated DMSO molecule exhibit the same type of hydrogen bonds to O1, O4 and O5 in neighboring molecules (see Table 2 for symmetry operators and numerical values). The exact bond lengths for C14 vary slightly, a bond to O5 is broken and one to O4 significantly elongated for molecule *B*, but the overall hydrogen-bonding pattern for this DMSO fragment is very similar for both molecules *A* and *B*. This is not the case for the other significantly modulated DMSO molecule. For **3B**, three significant C—H...O interactions are observed, towards O1A, O3A and O4A of neighboring entities. None of these are found for **3A**. All hydrogen-to-oxygen distances are beyond what could be still regarded as attractive and stabilizing. Methyl carbon atom

C16A is at a distance of 3.128 Å from O1B, close enough for a C—H...O hydrogen bond to be suspected, but its hydrogen atoms are rotated such that the H...O distances are > 2.8 Å, and the C—H...O angles are unfavorable at 97.9 and 99.5° (H-atom positions were clearly resolved in difference-density maps and were allowed to rotate to fit the experimental electron density). The shortest distance involving the H atoms of C16A is instead towards C1B of a neighboring catecholate ring (2.734 Å, shown as a green dashed line in Fig. 7), and C15A does not exhibit any H...X contacts < 2.8 Å. This clear difference between the hydrogen-bonding interactions of C15 and C16 in the two molecules is clearly related to the modulation that breaks the exact *Pbca* glide symmetry in the structure of **3**. It is not clear whether the ability to form stronger interactions is the cause for the modulation, or whether the modulation causes the differences in intermolecular interactions and the modulation itself is caused by other less-directional forces such as dispersive interactions. Most likely the concerted effects of both modulation and intermolecular interactions reinforcing and stabilizing each other lead to the observed packing of the molecules.

4. Database survey

A database survey of titanium catecholate complexes reveals a plethora of homoleptic triscatecholates but only a few in monometallic assemblies. A search of the Cambridge Structural Database (CSD, Version 5.42, accessed Feb 2021; Groom *et al.*, 2016) yields, in addition to **2^{Et3NH}** (Borgias *et al.*, 1984), eleven other monocationic homoleptic triscatecholate titanium complexes with only one metal center: SUKNUK (Kwamen *et al.*, 2020), SUKQAT (Kwamen *et al.*, 2020), GOJMIC (Tinoco *et al.*, 2008), LEXQUD (Dong *et al.*, 2018), LEXRAK (Dong *et al.*, 2018), MAGLAK (Van Craen *et al.*, 2016), VEPJUW (Davis *et al.*, 2006), VEPKAD (Davis *et al.*, 2006), VILXIX (Hahn *et al.*, 1991), XIKLOV (Chen *et al.*, 2018), and YUPNEF (Johnson *et al.*, 2020).

The conversion of triscatecholate complexes to heteroleptic complexes has been observed previously, as the hydroxide-induced displacement of a catecholate ligand from **2^{Et3NH}** to form the bis-(μ -oxo-bridged) biscatecholate **4** exemplifies (Borgias *et al.*, 1984). Direct syntheses are also known (Sakata *et al.*, 2010). For example, treatment of titanium methoxide with a methanolic solution of catechol **1** under ambient conditions resulted in the formation of a dinuclear heteroleptic complex **5** with a mixture of catechol/catecholate and methanol/methanolate ligands (Bazhenova *et al.*, 2016). Notably both examples of these heteroleptic complexes are multinuclear. Complex **5** dissolved in DMF, however, and exchanges all methanol/methanolate for DMF and rearranges to form the mononuclear [biscatecholate-bis-DMF]titanium complex **6**, the DMF analogue of the title compound (CCDC 1489371; Bazhenova *et al.*, 2016). Neutral and monometallic complexes of this kind are exceedingly rare. A search of the CSD yielded complex **6** as the only other heteroleptic mononuclear, neutral bis-catecholate complex with TiO₆ metal coordination; complex **3** is only the second such complex.

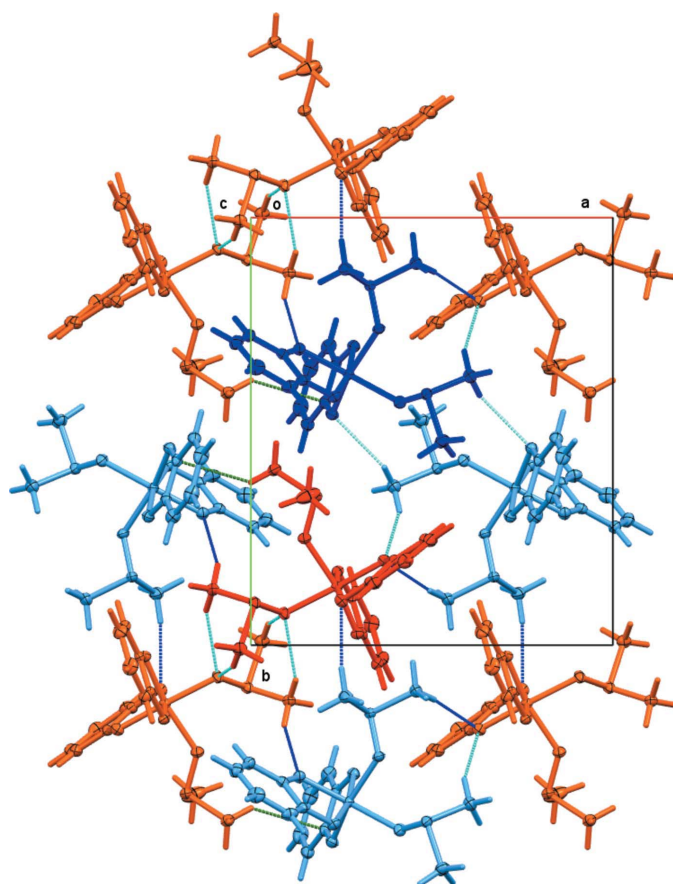


Figure 7

Directional interactions in **3**, viewed down the *c* axis. Red: molecule *A*, blue: molecule *B*. Lighter colored molecules are generated by crystal symmetry. Dark-blue dashed lines: C—H...O bonds with H...O distance < 2.5 Å; light-blue dashed lines: C—H...O bonds with H...O distance between 2.5 and 2.62 Å; green dashed lines C—H... π contacts. 50% probability ellipsoids.

5. Synthesis and crystallization

Triscatcholate **2^H** (500 mg, 1.34×10^{-3} mol), prepared as described in the literature (Davies & Dutremez, 1990), was dissolved at ~ 173 K, in the minimal amount of DMSO (~ 15 ml). The deep, dark-orange solution was allowed to cool slowly (in the water bath) to ambient temperature. The crystal mass that formed was broken up, placed on a porcelain frit, washed with minimal amount of cool DMSO (m.p. 292 K!), then cold diethyl ether, and dried under suction. The red-orange matted plates of **3** (320 mg, 0.76×10^{-3} mol, 57% yield) were analytically pure. By NMR spectroscopy (cf. Fig. 3B), the reaction is quantitative; nonetheless, no attempt was made to increase the yield by recovery of more product from the filtrate. $\text{C}_{16}\text{H}_{20}\text{O}_6\text{S}_2\text{Ti}$ ($M_w = 420.32$ g mol $^{-1}$); ^1H NMR (400 MHz, DMSO- d_6): δ 6.45 (*m*, 2H, 4,5-CH), 6.13 (*m*, 2H, 3,6-CH), 2.31 (*s*, 3H, CH $_3$) ppm; UV-vis (DMSO): λ_{max} (ϵ/M^{-1} cm $^{-1}$) = 280 (9000), 343 (2000), 441 (2500).

6. Refinement

Crystal data, data collection and structure refinement details are summarized in Table 3. The structure exhibits pseudo-orthorhombic symmetry (*Pbca*) and is twinned by a 180° rotation around the *a*- or *c*-axis. Application of the transformation matrix 1 0 0, 0 −1 0, 0 0 −1 yielded a twin ratio of 0.5399 (7):0.4401 (7). The pseudo-orthorhombic symmetry is broken by modulation of one of the catecholate rings by up to 1.4 Å, and one of the DMSO ligands by over 1.7 Å.

C—H bond distances were constrained to 0.95 Å for aromatic C—H and to 0.98 Å for aliphatic CH $_3$ moieties, respectively. $U_{\text{iso}}(\text{H})$ values were set to a multiple of $U_{\text{eq}}(\text{C})$ with 1.5 for CH $_3$ and 1.2 for C—H units. Reflections $\bar{1}12$, $11\bar{2}$ and 013 were affected by the beam stop and were omitted from the refinement.

Funding information

Funding for this research was provided by the National Science Foundation (grant No. CHE-1625543 to M. Zeller; grants No. CHE-1465133 and CHE-1800361 to C. Brückner).

References

- Albrecht, M., Burk, S. & Weis, P. (2008). *Synthesis*, pp. 2963–2967.
 Albrecht, M., Chen, X. & Van Craen, D. (2019). *Chem. Eur. J.* **25**, 4265–4273.
 Ali, N. J. & Milne, S. J. (1987). *British Ceram. Trans. J.* **86**, 113–117.
 Alvarez, S., Avnir, D., Llunell, M. & Pinsky, M. (2002). *New J. Chem.* **26**, 996–1009.
 Bazhenova, T. A., Kovaleva, N. V., Shilov, G. V., Petrova, G. N. & Kuznetsov, D. A. (2016). *Eur. J. Inorg. Chem.* pp. 5215–5221.
 Bobbitt, N. S. & Snurr, R. Q. (2018). *Ind. Eng. Chem. Res.* **57**, 17488–17495.
 Borgias, B. A., Cooper, S. R., Koh, Y. B. & Raymond, K. N. (1984). *Inorg. Chem.* **23**, 1009–1016.
 Brückner, C., Powers, R. E. & Raymond, K. N. (1998). *Angew. Chem. Int. Ed.* **37**, 1837–1839.
 Cao, J., Ma, W., Lyu, K., Zhuang, L., Cong, H. & Deng, H. (2020). *Chem. Sci.* **11**, 3978–3985.

Table 3

Experimental details.

Crystal data	
Chemical formula	[Ti(C ₆ H ₄ O ₂) ₂ (C ₂ H ₆ OS) ₂]
M_r	420.34
Crystal system, space group	Monoclinic, $P2_1/c$
Temperature (K)	100
a , b , c (Å)	12.4531 (3), 14.7287 (3), 20.3676 (5)
β (°)	90.0445 (9)
V (Å ³)	3735.78 (15)
Z	8
Radiation type	Mo $K\alpha$
μ (mm ^{−1})	0.71
Crystal size (mm)	0.35 × 0.23 × 0.09
Data collection	
Diffraction meter	Nonius Kappa CCD
Absorption correction	Multi-scan (SCALEPACK; Otwinowski & Minor, 1997)
T_{min} , T_{max}	0.668, 0.939
No. of measured, independent and observed [$I > 2\sigma(I)$] reflections	39962, 8552, 7393
R_{int}	0.047
($\sin \theta/\lambda$) _{max} (Å ^{−1})	0.666
Refinement	
$R[F^2 > 2\sigma(F^2)]$, $wR(F^2)$, S	0.036, 0.073, 1.04
No. of reflections	8552
No. of parameters	461
H-atom treatment	H-atom parameters constrained
$\Delta\rho_{\text{max}}$, $\Delta\rho_{\text{min}}$ (e Å ^{−3})	0.41, −0.45

Computer programs: COLLECT (Nonius, 1998), HKL-3000 (Otwinowski & Minor, 1997), SHELXS97 (Sheldrick, 2008), SHELXL2018/3 (Sheldrick, 2015), ShelXle (Hübschle *et al.*, 2011), Mercury (Macrae *et al.*, 2020), and publCIF (Westrip, 2010).

- Casanova, D., Cirera, J., Llunell, M., Alemany, P., Avnir, D. & Alvarez, S. (2004). *J. Am. Chem. Soc.* **126**, 1755–1763.
 Caulder, D. L., Brückner, C., Powers, R. E., König, S., Parac, T. N., Leary, J. A. & Raymond, K. N. (2001). *J. Am. Chem. Soc.* **123**, 8923–8938.
 Chen, X., Gerger, T. M., Räuber, C., Raabe, G., Göb, C., Oppel, I. M. & Albrecht, M. (2018). *Angew. Chem. Int. Ed.* **57**, 11817–11820.
 Cirera, J., Ruiz, E. & Alvarez, S. (2005). *Organometallics*, **24**, 1556–1562.
 Davies, J. A. & Dutremez, S. (1990). *J. Am. Ceram. Soc.* **73**, 1429–1430.
 Davis, A. V., Firman, T. K., Hay, B. P. & Raymond, K. N. (2006). *J. Am. Chem. Soc.* **128**, 9484–9496.
 Dehaen, G., Eliseeva, S. V., Kimpe, K., Laurent, S., Vander Elst, L., Muller, R. N., Dehaen, W., Binnemans, K. & Parac-Vogt, T. N. (2012). *Chem. Eur. J.* **18**, 293–302.
 Dong, G.-L., Wang, L., Fang, W.-H. & Zhang, L. (2018). *Inorg. Chem. Commun.* **93**, 61–64.
 Groom, C. R., Bruno, I. J., Lightfoot, M. P. & Ward, S. C. (2016). *Acta Cryst. B72*, 171–179.
 Hahn, F. E., Rupprecht, S. & Moock, K. H. (1991). *J. Chem. Soc. Chem. Commun.* pp. 224–225.
 Hübschle, C. B., Sheldrick, G. M. & Dittrich, B. (2011). *J. Appl. Cryst.* **44**, 1281–1284.
 Johnson, S. H., Jackson, C. E. & Zadrozny, J. M. (2020). *Inorg. Chem.* **59**, 7479–7486.
 Kaim, W. & Schwederski, B. (2010). *Coord. Chem. Rev.* **254**, 1580–1588.
 Kwamen, A. C. N., Schlottmann, M., Van Craen, D., Isaak, E., Baums, J., Shen, L., Massomi, A., Räuber, C., Joseph, B. P., Raabe, G., Göb, C., Oppel, I. M., Puttreddy, R., Ward, J. S., Rissanen, K., Fröhlich, R. & Albrecht, M. (2020). *Chem. Eur. J.* **26**, 1396–1405.

- Macrae, C. F., Sovago, I., Cottrell, S. J., Galek, P. T. A., McCabe, P., Pidcock, E., Platings, M., Shields, G. P., Stevens, J. S., Towler, M. & Wood, P. A. (2020). *J. Appl. Cryst.* **53**, 226–235.
- Marteel-Parrish, A., DeCarlo, S., Harlan, D., Martin, J. & Sheridan, H. (2008). *Green Chem. Lett. Rev.* **1**, 197–203.
- Nguyen, N. T. T., Furukawa, H., Gándara, F., Trickett, C. A., Jeong, H. M., Cordova, K. E. & Yaghi, O. M. (2015). *J. Am. Chem. Soc.* **137**, 15394–15397.
- Nonius (1998). *COLLECT*. Nonius BV, Delft, The Netherlands.
- Otwinowski, Z. & Minor, W. (1997). *Methods in Enzymology*, Vol. 276, *Macromolecular Crystallography*, Part A, edited by C. W. Carter Jr & R. M. Sweet, pp. 307–326. New York: Academic Press.
- Passadis, S. S., Papanikolaou, M. G., Elliott, A., Tsiafoulis, C. G., Tshipis, A. C., Keramidas, A. D., Miras, H. N. & Kabanos, T. A. (2020). *Inorg. Chem.* **59**, 18345–18357.
- Pierpont, C. G. & Lange, C. W. (1994). *Prog. Inorg. Chem.* **41**, 331–442.
- Pinsky, M. & Avnir, D. (1998). *Inorg. Chem.* **37**, 5575–5582.
- Sakata, Y., Hiraoka, S. & Shionoya, M. (2010). *Chem. Eur. J.* **16**, 3318–3325.
- Sheldrick, G. M. (2008). *Acta Cryst. A* **64**, 112–122.
- Sheldrick, G. M. (2015). *Acta Cryst. C* **71**, 3–8.
- Sonström, A., Schneider, D., Maichle-Mössmer, C. & Anwender, R. (2019). *Eur. J. Inorg. Chem.* pp.682–692.
- Tinoco, A. D., Eames, E. V., Incarvito, C. D. & Valentine, A. M. (2008). *Inorg. Chem.* **47**, 8380–8390.
- Van Craen, D., Albrecht, M., Raabe, G., Pan, F. & Rissanen, K. (2016). *Chem. Eur. J.* **22**, 3255–3258.
- Westrip, S. P. (2010). *J. Appl. Cryst.* **43**, 920–925.

1 supporting information

2 Bis(catecholato- κ^2O,O')bis(dimethyl sulfoxide- κO)titanium(IV)

3 Nisansala Hewage, Carolyn Mastriano, Christian Brückner* and Matthias Zeller

4 Computing details

5 Data collection: *COLLECT* (Nonius, 1998); cell refinement: *HKL-3000* (Otwinowski & Minor, 1997); data reduction:
 6 *HKL-3000* (Otwinowski & Minor, 1997); program(s) used to solve structure: *SHELXS97* (Sheldrick, 2008); program(s)
 7 used to refine structure: *SHELXL2018/3* (Sheldrick, 2015), *ShelXle* (Hübschle *et al.*, 2011); molecular graphics: *Mercury*
 8 (Macrae *et al.*, 2020); software used to prepare material for publication: *publCIF* (Westrip, 2010).

9 Bis(benzene-1,2-diolato- κ^2O,O')bis(dimethyl sulfoxide- κO)titanium(IV)

10 Crystal data

11	[Ti(C ₆ H ₄ O ₂) ₂ (C ₂ H ₆ OS) ₂]	$F(000) = 1744$
12	$M_r = 420.34$	$D_x = 1.495 \text{ Mg m}^{-3}$
13	Monoclinic, $P2_1/c$	Mo $K\alpha$ radiation, $\lambda = 0.71073 \text{ \AA}$
14	$a = 12.4531 (3) \text{ \AA}$	Cell parameters from 39962 reflections
15	$b = 14.7287 (3) \text{ \AA}$	$\theta = 1.4\text{--}28.3^\circ$
16	$c = 20.3676 (5) \text{ \AA}$	$\mu = 0.71 \text{ mm}^{-1}$
17	$\beta = 90.0445 (9)^\circ$	$T = 100 \text{ K}$
18	$V = 3735.78 (15) \text{ \AA}^3$	Plate, orange
19	$Z = 8$	$0.35 \times 0.23 \times 0.09 \text{ mm}$

20 Data collection

21	Nonius Kappa CCD	39962 measured reflections
	diffractometer	8552 independent reflections
22	Radiation source: fine focus X-ray tube	7393 reflections with $I > 2\sigma(I)$
23	Graphite monochromator	$R_{\text{int}} = 0.047$
24	ω and ϕ scans	$\theta_{\text{max}} = 28.3^\circ$, $\theta_{\text{min}} = 1.4^\circ$
25	Absorption correction: multi-scan	$h = -16 \rightarrow 14$
	(<i>SCALEPACK</i> ; Otwinowski & Minor, 1997)	$k = -19 \rightarrow 18$
26	$T_{\text{min}} = 0.668$, $T_{\text{max}} = 0.939$	$l = -25 \rightarrow 27$

27 Refinement

28	Refinement on F^2	Hydrogen site location: inferred from
29	Least-squares matrix: full	neighbouring sites
30	$R[F^2 > 2\sigma(F^2)] = 0.036$	H-atom parameters constrained
31	$wR(F^2) = 0.073$	$w = 1/[\sigma^2(F_o^2) + (0.0246P)^2 + 2.3086P]$
32	$S = 1.04$	where $P = (F_o^2 + 2F_c^2)/3$
33	8552 reflections	$(\Delta/\sigma)_{\text{max}} = 0.001$
34	461 parameters	$\Delta\rho_{\text{max}} = 0.41 \text{ e \AA}^{-3}$
35	0 restraints	$\Delta\rho_{\text{min}} = -0.45 \text{ e \AA}^{-3}$
36	Primary atom site location: structure-invariant	Extinction correction: <i>SHELXL2018/3</i>
	direct methods	(Sheldrick 2015),
37	Secondary atom site location: difference Fourier	$\text{Fc}^* = k\text{Fc}[1 + 0.001 \times \text{Fc}^2 \lambda^3 / \sin(2\theta)]^{-1/4}$
	map	Extinction coefficient: 0.00192 (16)

38 *Special details*

39 **Geometry.** All e.s.d.'s (except the e.s.d. in the dihedral angle between two l.s. planes) are estimated using the full
covariance matrix. The cell e.s.d.'s are taken into account individually in the estimation of e.s.d.'s in distances, angles and
torsion angles; correlations between e.s.d.'s in cell parameters are only used when they are defined by crystal symmetry.
An approximate (isotropic) treatment of cell e.s.d.'s is used for estimating e.s.d.'s involving l.s. planes.

40 **Refinement.** The structure exhibits pseudo-orthorhombic symmetry (Pbca) and is twinned by a 180 degree rotation
around the *a* or *c* axis. Application of the twin matrix 1 0 0, 0 – 1 0, 0 0 – 1 yielded a twin ratio of 0.5399 (7) to
0.4401 (7). The pseudo-orthorhombic symmetry is broken by modulation of the phenylene rings by up to 1.4 Angstrom.

41 *Fractional atomic coordinates and isotropic or equivalent isotropic displacement parameters (\AA^2)*

	<i>x</i>	<i>y</i>	<i>z</i>	$U_{\text{iso}}^*/U_{\text{eq}}$
43 Ti1A	0.23792 (4)	0.86347 (3)	0.47159 (2)	0.01639 (11)
44 S1A	0.01041 (6)	0.90084 (4)	0.40944 (3)	0.01861 (14)
45 S2A	0.17900 (6)	0.65300 (4)	0.43411 (4)	0.02237 (15)
46 O1A	0.29396 (14)	0.97324 (11)	0.50941 (9)	0.0181 (4)
47 O2A	0.23951 (14)	0.82784 (11)	0.56301 (8)	0.0186 (4)
48 O3A	0.24928 (15)	0.89650 (11)	0.37882 (9)	0.0199 (4)
49 O4A	0.36941 (15)	0.80282 (12)	0.45119 (9)	0.0196 (4)
50 O5A	0.09197 (14)	0.92578 (12)	0.46412 (9)	0.0193 (4)
51 O6A	0.14803 (15)	0.75007 (12)	0.45420 (9)	0.0220 (4)
52 C1A	0.3082 (2)	0.97271 (16)	0.57562 (13)	0.0171 (5)
53 C2A	0.3488 (2)	1.04342 (17)	0.61292 (13)	0.0208 (5)
54 H2A	0.368091	1.099281	0.592823	0.025*
55 C3A	0.3608 (2)	1.03143 (19)	0.68025 (14)	0.0278 (6)
56 H3A	0.388467	1.079614	0.706268	0.033*
57 C4A	0.3331 (3)	0.9502 (2)	0.70978 (15)	0.0293 (7)
58 H4A	0.342127	0.943114	0.755821	0.035*
59 C5A	0.2919 (2)	0.87832 (18)	0.67256 (14)	0.0246 (6)
60 H5A	0.273006	0.822531	0.692909	0.030*
61 C6A	0.2790 (2)	0.89005 (17)	0.60499 (13)	0.0169 (5)
62 C7A	0.3287 (2)	0.85289 (16)	0.34636 (13)	0.0186 (5)
63 C8A	0.3427 (2)	0.85377 (18)	0.27873 (13)	0.0249 (6)
64 H8A	0.296315	0.887824	0.251048	0.030*
65 C9A	0.4274 (2)	0.80286 (19)	0.25277 (14)	0.0270 (6)
66 H9A	0.437837	0.801484	0.206588	0.032*
67 C10A	0.4962 (2)	0.75445 (18)	0.29301 (14)	0.0269 (6)
68 H10A	0.553816	0.721326	0.274072	0.032*
69 C11A	0.4823 (2)	0.75350 (17)	0.36086 (14)	0.0230 (6)
70 H11A	0.530330	0.721273	0.388597	0.028*
71 C12A	0.3960 (2)	0.80109 (17)	0.38657 (13)	0.0179 (5)
72 C13A	–0.0307 (2)	1.00875 (18)	0.37881 (14)	0.0231 (6)
73 H13A	–0.094276	1.001230	0.350983	0.035*
74 H13B	0.027660	1.035434	0.352935	0.035*
75 H13C	–0.047955	1.048911	0.415678	0.035*
76 C14A	–0.1055 (2)	0.86991 (17)	0.45376 (14)	0.0219 (6)
77 H14A	–0.165463	0.861017	0.423232	0.033*
78 H14B	–0.123587	0.918174	0.484975	0.033*

79	H14C	-0.091925	0.813351	0.477709	0.033*
80	C15A	0.1571 (3)	0.6507 (2)	0.34776 (16)	0.0470 (10)
81	H15A	0.164735	0.588285	0.331680	0.070*
82	H15B	0.209848	0.689715	0.325975	0.070*
83	H15C	0.084493	0.672688	0.338069	0.070*
84	C16A	0.0645 (2)	0.58991 (18)	0.45798 (15)	0.0267 (6)
85	H16A	0.069675	0.528144	0.440385	0.040*
86	H16B	-0.000313	0.619270	0.440775	0.040*
87	H16C	0.060692	0.587406	0.506008	0.040*
88	Ti1B	0.26978 (4)	0.36710 (3)	0.47110 (2)	0.01648 (10)
89	S1B	0.48538 (6)	0.41289 (4)	0.39989 (3)	0.01951 (14)
90	S2B	0.32921 (5)	0.15962 (4)	0.44898 (3)	0.01756 (14)
91	O1B	0.22436 (15)	0.46008 (11)	0.53031 (9)	0.0204 (4)
92	O2B	0.28384 (14)	0.30116 (11)	0.55326 (9)	0.0195 (4)
93	O3B	0.22962 (15)	0.41888 (11)	0.38620 (9)	0.0190 (4)
94	O4B	0.13334 (14)	0.30782 (12)	0.45810 (9)	0.0193 (4)
95	O5B	0.41145 (15)	0.43189 (12)	0.45889 (9)	0.0213 (4)
96	O6B	0.35320 (15)	0.26045 (11)	0.43304 (9)	0.0197 (4)
97	C1B	0.2044 (2)	0.43151 (18)	0.59244 (13)	0.0190 (5)
98	C2B	0.1564 (2)	0.48346 (19)	0.64125 (14)	0.0252 (6)
99	H2B	0.137199	0.544949	0.633482	0.030*
100	C3B	0.1374 (3)	0.4429 (2)	0.70182 (15)	0.0318 (7)
101	H3B	0.105239	0.477313	0.736001	0.038*
102	C4B	0.1645 (2)	0.3529 (2)	0.71306 (14)	0.0306 (7)
103	H4B	0.148461	0.325989	0.754284	0.037*
104	C5B	0.2149 (2)	0.30157 (19)	0.66489 (13)	0.0264 (6)
105	H5B	0.235155	0.240446	0.673191	0.032*
106	C6B	0.2353 (2)	0.34154 (17)	0.60413 (13)	0.0201 (5)
107	C7B	0.1430 (2)	0.38045 (16)	0.35732 (13)	0.0189 (6)
108	C8B	0.1074 (2)	0.39564 (18)	0.29362 (14)	0.0248 (6)
109	H8B	0.145005	0.435848	0.265315	0.030*
110	C9B	0.0150 (3)	0.35044 (19)	0.27199 (14)	0.0295 (6)
111	H9B	-0.009738	0.360043	0.228406	0.035*
112	C10B	-0.0408 (2)	0.29247 (18)	0.31242 (14)	0.0256 (6)
113	H10B	-0.103731	0.263272	0.296679	0.031*
114	C11B	-0.0054 (2)	0.27610 (17)	0.37675 (13)	0.0221 (6)
115	H11B	-0.043914	0.236415	0.404958	0.027*
116	C12B	0.0873 (2)	0.31931 (17)	0.39817 (13)	0.0176 (5)
117	C13B	0.5285 (3)	0.52345 (18)	0.37659 (15)	0.0271 (7)
118	H13D	0.584170	0.518513	0.342780	0.041*
119	H13E	0.557799	0.555009	0.414997	0.041*
120	H13F	0.467374	0.557725	0.359159	0.041*
121	C14B	0.6051 (2)	0.37109 (19)	0.43729 (16)	0.0274 (7)
122	H14D	0.659787	0.361118	0.403503	0.041*
123	H14E	0.589689	0.313647	0.459669	0.041*
124	H14F	0.631484	0.415538	0.469258	0.041*
125	C15B	0.2614 (2)	0.12076 (17)	0.37805 (14)	0.0271 (6)
126	H15D	0.250241	0.055054	0.381248	0.041*

127	H15E	0.304702	0.134322	0.339095	0.041*
128	H15F	0.191809	0.151379	0.374497	0.041*
129	C16B	0.4557 (2)	0.10696 (18)	0.43641 (15)	0.0243 (6)
130	H16D	0.447454	0.040889	0.439005	0.036*
131	H16E	0.506156	0.127350	0.470277	0.036*
132	H16F	0.483304	0.123567	0.392994	0.036*

133 *Atomic displacement parameters (\AA^2)*

		U^{11}	U^{22}	U^{33}	U^{12}	U^{13}	U^{23}
134							
135	Ti1A	0.0163 (3)	0.0142 (2)	0.0187 (2)	0.00011 (18)	−0.0001 (2)	−0.00122 (16)
136	S1A	0.0179 (3)	0.0183 (3)	0.0196 (3)	0.0017 (2)	−0.0006 (3)	−0.0031 (2)
137	S2A	0.0197 (4)	0.0154 (3)	0.0319 (4)	−0.0009 (2)	0.0018 (3)	0.0002 (3)
138	O1A	0.0205 (10)	0.0161 (9)	0.0175 (9)	−0.0006 (7)	−0.0004 (7)	0.0008 (7)
139	O2A	0.0190 (10)	0.0166 (8)	0.0203 (9)	−0.0029 (7)	0.0006 (8)	−0.0004 (7)
140	O3A	0.0197 (10)	0.0204 (9)	0.0197 (9)	0.0040 (7)	−0.0002 (8)	0.0006 (7)
141	O4A	0.0210 (10)	0.0191 (9)	0.0188 (9)	0.0022 (7)	0.0007 (8)	0.0000 (7)
142	O5A	0.0159 (10)	0.0202 (9)	0.0218 (10)	0.0022 (7)	−0.0018 (8)	−0.0061 (8)
143	O6A	0.0213 (10)	0.0171 (9)	0.0276 (10)	−0.0012 (7)	−0.0001 (8)	−0.0050 (7)
144	C1A	0.0117 (13)	0.0177 (12)	0.0219 (13)	0.0041 (9)	0.0000 (10)	−0.0002 (10)
145	C2A	0.0173 (14)	0.0182 (12)	0.0271 (14)	−0.0019 (10)	−0.0020 (11)	−0.0010 (10)
146	C3A	0.0283 (16)	0.0273 (14)	0.0278 (15)	−0.0022 (11)	−0.0078 (13)	−0.0059 (12)
147	C4A	0.0307 (18)	0.0382 (17)	0.0190 (14)	−0.0020 (13)	−0.0057 (12)	−0.0028 (12)
148	C5A	0.0209 (15)	0.0271 (14)	0.0258 (15)	−0.0015 (11)	−0.0005 (12)	0.0052 (11)
149	C6A	0.0117 (13)	0.0180 (12)	0.0210 (13)	0.0007 (10)	−0.0013 (10)	−0.0019 (10)
150	C7A	0.0184 (15)	0.0159 (12)	0.0216 (13)	−0.0028 (10)	0.0029 (11)	−0.0005 (10)
151	C8A	0.0292 (17)	0.0238 (14)	0.0217 (14)	−0.0046 (11)	−0.0008 (12)	0.0023 (11)
152	C9A	0.0316 (17)	0.0285 (15)	0.0209 (15)	−0.0051 (12)	0.0087 (12)	−0.0040 (11)
153	C10A	0.0252 (15)	0.0231 (13)	0.0323 (16)	−0.0037 (12)	0.0075 (13)	−0.0041 (12)
154	C11A	0.0191 (15)	0.0178 (13)	0.0322 (15)	−0.0003 (11)	0.0035 (12)	−0.0019 (11)
155	C12A	0.0177 (14)	0.0158 (12)	0.0203 (14)	−0.0032 (10)	0.0017 (11)	−0.0010 (10)
156	C13A	0.0253 (16)	0.0236 (14)	0.0205 (15)	−0.0002 (11)	0.0004 (12)	0.0046 (11)
157	C14A	0.0199 (14)	0.0179 (13)	0.0280 (15)	0.0000 (10)	0.0008 (12)	0.0013 (11)
158	C15A	0.076 (3)	0.0343 (18)	0.0308 (18)	−0.0207 (17)	0.0158 (18)	−0.0095 (14)
159	C16A	0.0244 (15)	0.0186 (13)	0.0372 (17)	−0.0038 (11)	0.0053 (13)	−0.0019 (12)
160	Ti1B	0.0168 (2)	0.0141 (2)	0.0185 (2)	0.00012 (18)	0.0016 (2)	0.00020 (17)
161	S1B	0.0187 (3)	0.0180 (3)	0.0219 (3)	−0.0023 (3)	0.0019 (3)	−0.0018 (2)
162	S2B	0.0156 (3)	0.0140 (3)	0.0231 (3)	−0.0003 (2)	0.0016 (3)	0.0003 (2)
163	O1B	0.0216 (10)	0.0173 (8)	0.0224 (10)	0.0025 (7)	0.0018 (8)	0.0000 (7)
164	O2B	0.0204 (10)	0.0179 (9)	0.0202 (10)	0.0010 (7)	−0.0002 (8)	−0.0007 (7)
165	O3B	0.0204 (10)	0.0174 (8)	0.0193 (9)	−0.0031 (7)	0.0009 (8)	0.0014 (7)
166	O4B	0.0191 (10)	0.0207 (9)	0.0180 (9)	−0.0003 (7)	0.0006 (8)	0.0037 (7)
167	O5B	0.0206 (10)	0.0208 (10)	0.0226 (10)	−0.0010 (7)	0.0055 (9)	−0.0047 (8)
168	O6B	0.0205 (10)	0.0131 (8)	0.0256 (10)	−0.0024 (7)	0.0059 (8)	−0.0012 (7)
169	C1B	0.0168 (14)	0.0219 (13)	0.0182 (13)	−0.0019 (10)	0.0028 (10)	−0.0037 (10)
170	C2B	0.0211 (15)	0.0256 (14)	0.0289 (15)	0.0000 (11)	0.0003 (12)	−0.0067 (11)
171	C3B	0.0296 (18)	0.0444 (18)	0.0215 (15)	−0.0053 (14)	0.0052 (13)	−0.0102 (13)
172	C4B	0.0297 (17)	0.0444 (18)	0.0176 (14)	−0.0072 (13)	0.0008 (12)	−0.0036 (12)

173	C5B	0.0285 (16)	0.0293 (15)	0.0213 (14)	−0.0049 (11)	−0.0020 (12)	0.0026 (11)
174	C6B	0.0149 (13)	0.0254 (13)	0.0201 (13)	−0.0024 (10)	−0.0019 (11)	−0.0056 (11)
175	C7B	0.0215 (15)	0.0143 (12)	0.0210 (13)	0.0007 (10)	0.0011 (11)	−0.0016 (10)
176	C8B	0.0335 (17)	0.0217 (14)	0.0190 (14)	−0.0026 (11)	0.0032 (12)	0.0034 (11)
177	C9B	0.0386 (18)	0.0305 (15)	0.0195 (14)	−0.0009 (13)	−0.0054 (13)	−0.0029 (11)
178	C10B	0.0247 (16)	0.0260 (14)	0.0260 (15)	−0.0037 (11)	−0.0055 (12)	−0.0025 (11)
179	C11B	0.0211 (15)	0.0200 (13)	0.0252 (14)	−0.0020 (10)	0.0023 (12)	0.0002 (10)
180	C12B	0.0197 (14)	0.0164 (12)	0.0166 (13)	0.0030 (10)	0.0014 (11)	−0.0005 (10)
181	C13B	0.0288 (17)	0.0234 (14)	0.0290 (16)	−0.0050 (12)	−0.0016 (13)	0.0069 (12)
182	C14B	0.0231 (16)	0.0247 (15)	0.0344 (17)	0.0028 (11)	0.0018 (13)	0.0019 (13)
183	C15B	0.0273 (16)	0.0194 (13)	0.0347 (16)	−0.0006 (11)	−0.0076 (13)	−0.0025 (11)
184	C16B	0.0190 (15)	0.0219 (13)	0.0320 (16)	0.0024 (10)	0.0016 (12)	0.0026 (11)

185 *Geometric parameters (Å, °)*

186	Ti1A—O4A	1.9113 (19)	Ti1B—O1B	1.9108 (18)
187	Ti1A—O1A	1.9220 (17)	Ti1B—O4B	1.9284 (19)
188	Ti1A—O2A	1.9346 (18)	Ti1B—O2B	1.9427 (18)
189	Ti1A—O3A	1.9564 (18)	Ti1B—O3B	1.9545 (18)
190	Ti1A—O6A	2.0414 (18)	Ti1B—O5B	2.0214 (19)
191	Ti1A—O5A	2.0416 (18)	Ti1B—O6B	2.0367 (17)
192	S1A—O5A	1.5509 (19)	S1B—O5B	1.5400 (19)
193	S1A—C14A	1.763 (3)	S1B—C13B	1.779 (3)
194	S1A—C13A	1.782 (3)	S1B—C14B	1.783 (3)
195	S2A—O6A	1.5364 (19)	S2B—O6B	1.5494 (18)
196	S2A—C16A	1.771 (3)	S2B—C15B	1.768 (3)
197	S2A—C15A	1.780 (3)	S2B—C16B	1.774 (3)
198	O1A—C1A	1.360 (3)	O1B—C1B	1.357 (3)
199	O2A—C6A	1.346 (3)	O2B—C6B	1.339 (3)
200	O3A—C7A	1.352 (3)	O3B—C7B	1.353 (3)
201	O4A—C12A	1.358 (3)	O4B—C12B	1.359 (3)
202	C1A—C2A	1.384 (4)	C1B—C2B	1.390 (4)
203	C1A—C6A	1.404 (3)	C1B—C6B	1.400 (4)
204	C2A—C3A	1.391 (4)	C2B—C3B	1.392 (4)
205	C2A—H2A	0.9500	C2B—H2B	0.9500
206	C3A—C4A	1.383 (4)	C3B—C4B	1.387 (4)
207	C3A—H3A	0.9500	C3B—H3B	0.9500
208	C4A—C5A	1.399 (4)	C4B—C5B	1.389 (4)
209	C4A—H4A	0.9500	C4B—H4B	0.9500
210	C5A—C6A	1.396 (4)	C5B—C6B	1.394 (4)
211	C5A—H5A	0.9500	C5B—H5B	0.9500
212	C7A—C8A	1.389 (4)	C7B—C8B	1.389 (4)
213	C7A—C12A	1.398 (4)	C7B—C12B	1.409 (4)
214	C8A—C9A	1.398 (4)	C8B—C9B	1.401 (4)
215	C8A—H8A	0.9500	C8B—H8B	0.9500
216	C9A—C10A	1.383 (4)	C9B—C10B	1.375 (4)
217	C9A—H9A	0.9500	C9B—H9B	0.9500
218	C10A—C11A	1.393 (4)	C10B—C11B	1.403 (4)

219	C10A—H10A	0.9500	C10B—H10B	0.9500
220	C11A—C12A	1.385 (4)	C11B—C12B	1.388 (4)
221	C11A—H11A	0.9500	C11B—H11B	0.9500
222	C13A—H13A	0.9800	C13B—H13D	0.9800
223	C13A—H13B	0.9800	C13B—H13E	0.9800
224	C13A—H13C	0.9800	C13B—H13F	0.9800
225	C14A—H14A	0.9800	C14B—H14D	0.9800
226	C14A—H14B	0.9800	C14B—H14E	0.9800
227	C14A—H14C	0.9800	C14B—H14F	0.9800
228	C15A—H15A	0.9800	C15B—H15D	0.9800
229	C15A—H15B	0.9800	C15B—H15E	0.9800
230	C15A—H15C	0.9800	C15B—H15F	0.9800
231	C16A—H16A	0.9800	C16B—H16D	0.9800
232	C16A—H16B	0.9800	C16B—H16E	0.9800
233	C16A—H16C	0.9800	C16B—H16F	0.9800
234				
235	O4A—Ti1A—O1A	99.75 (8)	O1B—Ti1B—O4B	98.62 (8)
236	O4A—Ti1A—O2A	94.27 (8)	O1B—Ti1B—O2B	80.85 (8)
237	O1A—Ti1A—O2A	80.73 (7)	O4B—Ti1B—O2B	88.32 (8)
238	O4A—Ti1A—O3A	81.00 (8)	O1B—Ti1B—O3B	101.72 (8)
239	O1A—Ti1A—O3A	98.71 (8)	O4B—Ti1B—O3B	80.24 (8)
240	O2A—Ti1A—O3A	175.09 (8)	O2B—Ti1B—O3B	168.52 (8)
241	O4A—Ti1A—O6A	92.85 (8)	O1B—Ti1B—O5B	89.89 (8)
242	O1A—Ti1A—O6A	163.08 (8)	O4B—Ti1B—O5B	165.00 (8)
243	O2A—Ti1A—O6A	87.15 (7)	O2B—Ti1B—O5B	105.30 (8)
244	O3A—Ti1A—O6A	94.35 (8)	O3B—Ti1B—O5B	85.97 (8)
245	O4A—Ti1A—O5A	163.07 (8)	O1B—Ti1B—O6B	160.77 (8)
246	O1A—Ti1A—O5A	88.55 (7)	O4B—Ti1B—O6B	92.76 (8)
247	O2A—Ti1A—O5A	101.66 (8)	O2B—Ti1B—O6B	84.07 (7)
248	O3A—Ti1A—O5A	83.18 (8)	O3B—Ti1B—O6B	95.42 (8)
249	O6A—Ti1A—O5A	82.35 (7)	O5B—Ti1B—O6B	82.64 (7)
250	O5A—S1A—C14A	103.27 (12)	O5B—S1B—C13B	102.87 (13)
251	O5A—S1A—C13A	103.16 (12)	O5B—S1B—C14B	103.27 (13)
252	C14A—S1A—C13A	100.06 (13)	C13B—S1B—C14B	100.22 (14)
253	O6A—S2A—C16A	102.29 (12)	O6B—S2B—C15B	103.36 (12)
254	O6A—S2A—C15A	104.06 (14)	O6B—S2B—C16B	102.56 (12)
255	C16A—S2A—C15A	97.94 (16)	C15B—S2B—C16B	99.43 (14)
256	C1A—O1A—Ti1A	116.08 (15)	C1B—O1B—Ti1B	114.90 (15)
257	C6A—O2A—Ti1A	115.48 (15)	C6B—O2B—Ti1B	113.83 (15)
258	C7A—O3A—Ti1A	114.05 (15)	C7B—O3B—Ti1B	115.14 (15)
259	C12A—O4A—Ti1A	115.43 (16)	C12B—O4B—Ti1B	115.97 (16)
260	S1A—O5A—Ti1A	121.98 (10)	S1B—O5B—Ti1B	122.18 (11)
261	S2A—O6A—Ti1A	132.05 (11)	S2B—O6B—Ti1B	124.13 (11)
262	O1A—C1A—C2A	125.9 (2)	O1B—C1B—C2B	125.1 (2)
263	O1A—C1A—C6A	113.2 (2)	O1B—C1B—C6B	113.7 (2)
264	C2A—C1A—C6A	120.8 (2)	C2B—C1B—C6B	121.2 (2)
265	C1A—C2A—C3A	119.0 (2)	C1B—C2B—C3B	118.1 (3)
266	C1A—C2A—H2A	120.5	C1B—C2B—H2B	120.9

267	C3A—C2A—H2A	120.5	C3B—C2B—H2B	120.9
268	C4A—C3A—C2A	120.8 (3)	C4B—C3B—C2B	121.0 (3)
269	C4A—C3A—H3A	119.6	C4B—C3B—H3B	119.5
270	C2A—C3A—H3A	119.6	C2B—C3B—H3B	119.5
271	C3A—C4A—C5A	120.7 (3)	C3B—C4B—C5B	120.9 (3)
272	C3A—C4A—H4A	119.7	C3B—C4B—H4B	119.5
273	C5A—C4A—H4A	119.7	C5B—C4B—H4B	119.5
274	C6A—C5A—C4A	118.8 (3)	C4B—C5B—C6B	118.7 (3)
275	C6A—C5A—H5A	120.6	C4B—C5B—H5B	120.7
276	C4A—C5A—H5A	120.6	C6B—C5B—H5B	120.7
277	O2A—C6A—C5A	125.7 (2)	O2B—C6B—C5B	125.6 (2)
278	O2A—C6A—C1A	114.5 (2)	O2B—C6B—C1B	114.4 (2)
279	C5A—C6A—C1A	119.9 (2)	C5B—C6B—C1B	120.0 (2)
280	O3A—C7A—C8A	125.0 (2)	O3B—C7B—C8B	126.3 (2)
281	O3A—C7A—C12A	114.3 (2)	O3B—C7B—C12B	113.8 (2)
282	C8A—C7A—C12A	120.7 (3)	C8B—C7B—C12B	119.9 (2)
283	C7A—C8A—C9A	117.7 (3)	C7B—C8B—C9B	118.6 (2)
284	C7A—C8A—H8A	121.1	C7B—C8B—H8B	120.7
285	C9A—C8A—H8A	121.1	C9B—C8B—H8B	120.7
286	C10A—C9A—C8A	121.3 (3)	C10B—C9B—C8B	121.5 (3)
287	C10A—C9A—H9A	119.3	C10B—C9B—H9B	119.3
288	C8A—C9A—H9A	119.3	C8B—C9B—H9B	119.3
289	C9A—C10A—C11A	121.0 (3)	C9B—C10B—C11B	120.5 (3)
290	C9A—C10A—H10A	119.5	C9B—C10B—H10B	119.7
291	C11A—C10A—H10A	119.5	C11B—C10B—H10B	119.7
292	C12A—C11A—C10A	117.8 (3)	C12B—C11B—C10B	118.4 (2)
293	C12A—C11A—H11A	121.1	C12B—C11B—H11B	120.8
294	C10A—C11A—H11A	121.1	C10B—C11B—H11B	120.8
295	O4A—C12A—C11A	124.5 (2)	O4B—C12B—C11B	125.1 (2)
296	O4A—C12A—C7A	114.3 (2)	O4B—C12B—C7B	113.8 (2)
297	C11A—C12A—C7A	121.3 (3)	C11B—C12B—C7B	121.1 (2)
298	S1A—C13A—H13A	109.5	S1B—C13B—H13D	109.5
299	S1A—C13A—H13B	109.5	S1B—C13B—H13E	109.5
300	H13A—C13A—H13B	109.5	H13D—C13B—H13E	109.5
301	S1A—C13A—H13C	109.5	S1B—C13B—H13F	109.5
302	H13A—C13A—H13C	109.5	H13D—C13B—H13F	109.5
303	H13B—C13A—H13C	109.5	H13E—C13B—H13F	109.5
304	S1A—C14A—H14A	109.5	S1B—C14B—H14D	109.5
305	S1A—C14A—H14B	109.5	S1B—C14B—H14E	109.5
306	H14A—C14A—H14B	109.5	H14D—C14B—H14E	109.5
307	S1A—C14A—H14C	109.5	S1B—C14B—H14F	109.5
308	H14A—C14A—H14C	109.5	H14D—C14B—H14F	109.5
309	H14B—C14A—H14C	109.5	H14E—C14B—H14F	109.5
310	S2A—C15A—H15A	109.5	S2B—C15B—H15D	109.5
311	S2A—C15A—H15B	109.5	S2B—C15B—H15E	109.5
312	H15A—C15A—H15B	109.5	H15D—C15B—H15E	109.5
313	S2A—C15A—H15C	109.5	S2B—C15B—H15F	109.5
314	H15A—C15A—H15C	109.5	H15D—C15B—H15F	109.5

315	H15B—C15A—H15C	109.5	H15E—C15B—H15F	109.5
316	S2A—C16A—H16A	109.5	S2B—C16B—H16D	109.5
317	S2A—C16A—H16B	109.5	S2B—C16B—H16E	109.5
318	H16A—C16A—H16B	109.5	H16D—C16B—H16E	109.5
319	S2A—C16A—H16C	109.5	S2B—C16B—H16F	109.5
320	H16A—C16A—H16C	109.5	H16D—C16B—H16F	109.5
321	H16B—C16A—H16C	109.5	H16E—C16B—H16F	109.5
322				
323	C14A—S1A—O5A—Ti1A	123.30 (13)	C13B—S1B—O5B—Ti1B	137.68 (14)
324	C13A—S1A—O5A—Ti1A	−132.84 (14)	C14B—S1B—O5B—Ti1B	−118.38 (14)
325	C16A—S2A—O6A—Ti1A	159.79 (16)	C15B—S2B—O6B—Ti1B	103.47 (15)
326	C15A—S2A—O6A—Ti1A	−98.66 (19)	C16B—S2B—O6B—Ti1B	−153.50 (14)
327	Ti1A—O1A—C1A—C2A	179.0 (2)	Ti1B—O1B—C1B—C2B	−170.4 (2)
328	Ti1A—O1A—C1A—C6A	0.2 (3)	Ti1B—O1B—C1B—C6B	8.6 (3)
329	O1A—C1A—C2A—C3A	−178.5 (3)	O1B—C1B—C2B—C3B	177.3 (3)
330	C6A—C1A—C2A—C3A	0.3 (4)	C6B—C1B—C2B—C3B	−1.6 (4)
331	C1A—C2A—C3A—C4A	0.1 (4)	C1B—C2B—C3B—C4B	−0.6 (4)
332	C2A—C3A—C4A—C5A	−0.2 (5)	C2B—C3B—C4B—C5B	2.2 (5)
333	C3A—C4A—C5A—C6A	−0.1 (4)	C3B—C4B—C5B—C6B	−1.7 (4)
334	Ti1A—O2A—C6A—C5A	−177.4 (2)	Ti1B—O2B—C6B—C5B	166.9 (2)
335	Ti1A—O2A—C6A—C1A	2.8 (3)	Ti1B—O2B—C6B—C1B	−13.3 (3)
336	C4A—C5A—C6A—O2A	−179.2 (3)	C4B—C5B—C6B—O2B	179.4 (3)
337	C4A—C5A—C6A—C1A	0.5 (4)	C4B—C5B—C6B—C1B	−0.4 (4)
338	O1A—C1A—C6A—O2A	−1.9 (3)	O1B—C1B—C6B—O2B	3.2 (3)
339	C2A—C1A—C6A—O2A	179.2 (2)	C2B—C1B—C6B—O2B	−177.7 (2)
340	O1A—C1A—C6A—C5A	178.3 (2)	O1B—C1B—C6B—C5B	−176.9 (2)
341	C2A—C1A—C6A—C5A	−0.6 (4)	C2B—C1B—C6B—C5B	2.1 (4)
342	Ti1A—O3A—C7A—C8A	169.6 (2)	Ti1B—O3B—C7B—C8B	−170.3 (2)
343	Ti1A—O3A—C7A—C12A	−7.5 (3)	Ti1B—O3B—C7B—C12B	9.2 (3)
344	O3A—C7A—C8A—C9A	−178.2 (2)	O3B—C7B—C8B—C9B	−179.3 (3)
345	C12A—C7A—C8A—C9A	−1.3 (4)	C12B—C7B—C8B—C9B	1.2 (4)
346	C7A—C8A—C9A—C10A	−1.1 (4)	C7B—C8B—C9B—C10B	0.4 (4)
347	C8A—C9A—C10A—C11A	1.1 (4)	C8B—C9B—C10B—C11B	−0.8 (4)
348	C9A—C10A—C11A—C12A	1.3 (4)	C9B—C10B—C11B—C12B	−0.4 (4)
349	Ti1A—O4A—C12A—C11A	−173.6 (2)	Ti1B—O4B—C12B—C11B	173.9 (2)
350	Ti1A—O4A—C12A—C7A	6.8 (3)	Ti1B—O4B—C12B—C7B	−5.8 (3)
351	C10A—C11A—C12A—O4A	176.7 (2)	C10B—C11B—C12B—O4B	−177.6 (2)
352	C10A—C11A—C12A—C7A	−3.7 (4)	C10B—C11B—C12B—C7B	2.0 (4)
353	O3A—C7A—C12A—O4A	0.6 (3)	O3B—C7B—C12B—O4B	−2.3 (3)
354	C8A—C7A—C12A—O4A	−176.6 (2)	C8B—C7B—C12B—O4B	177.2 (2)
355	O3A—C7A—C12A—C11A	−179.0 (2)	O3B—C7B—C12B—C11B	178.0 (2)
356	C8A—C7A—C12A—C11A	3.8 (4)	C8B—C7B—C12B—C11B	−2.4 (4)

357 *Hydrogen-bond geometry (Å, °)*

358	<i>D</i> —H \cdots <i>A</i>	<i>D</i> —H	H \cdots <i>A</i>	<i>D</i> \cdots <i>A</i>	<i>D</i> —H \cdots <i>A</i>
359	C11A—H11A \cdots O2B ⁱ	0.95	2.62	3.491 (3)	153
360	C13A—H13C \cdots O5A ⁱⁱ	0.98	2.54	3.428 (3)	151

361	C14 <i>A</i> —H14 <i>B</i> ···O1 <i>A</i> ⁱⁱ	0.98	2.66	3.378 (3)	130
362	C14 <i>A</i> —H14 <i>B</i> ···O5 <i>A</i> ⁱⁱ	0.98	2.55	3.447 (3)	152
363	C14 <i>A</i> —H14 <i>C</i> ···O4 <i>B</i> ⁱⁱⁱ	0.98	2.27	3.193 (3)	156
364	C13 <i>B</i> —H13 <i>E</i> ···O5 <i>B</i> ⁱ	0.98	2.60	3.495 (4)	151
365	C14 <i>B</i> —H14 <i>E</i> ···O4 <i>A</i> ⁱ	0.98	2.55	3.438 (3)	151
366	C14 <i>B</i> —H14 <i>F</i> ···O1 <i>B</i> ⁱ	0.98	2.56	3.336 (3)	136
367	C15 <i>B</i> —H15 <i>D</i> ···O3 <i>A</i> ^{iv}	0.98	2.34	3.307 (3)	171
368	C16 <i>B</i> —H16 <i>D</i> ···O1 <i>A</i> ^{iv}	0.98	2.59	3.186 (3)	119
369	C16 <i>B</i> —H16 <i>E</i> ···O4 <i>A</i> ⁱ	0.98	2.45	3.427 (3)	173

370 Symmetry codes: (i) $-x+1, -y+1, -z+1$; (ii) $-x, -y+2, -z+1$; (iii) $-x, -y+1, -z+1$; (iv) $x, y-1, z$.

371 **other supporting information**

372 The following files will be made available to readers when your article is published. Unless otherwise stated, these files
373 will be the same as those submitted during the review process.

374 Crystal structure: contains datablock I. jy2018sup1.cif

375 Structure factors: contains datablock I. jy2018Isup2.hkl



ISSN: 2056-9890

YOU WILL AUTOMATICALLY BE SENT DETAILS OF HOW TO DOWNLOAD
AN ELECTRONIC REPRINT OF YOUR PAPER, FREE OF CHARGE.
PRINTED REPRINTS MAY BE PURCHASED USING THIS FORM.

Please scan your order and send to checkin@iucr.org

INTERNATIONAL UNION OF CRYSTALLOGRAPHY

5 Abbey Square
Chester CH1 2HU, England.

VAT No. GB 161 9034 76

Article No.: E220263-JY2018

Title of article Bis(catecholato- $\kappa^2 O, O'$)bis(dimethyl sulfoxide- κO)titanium(IV)

Name Christian Bruckner

Address Department of Chemistry, University of Connecticut, Storrs, CT 06269-3060, USA,

E-mail address (for electronic reprints) c.brockner@uconn.edu

DIGITAL PRINTED REPRINTS

I wish to order paid reprints

These reprints will be sent to the address given above. If the above address or e-mail address is not correct, please indicate an alternative:

--

PAYMENT

☐ An official purchase order made out to **INTERNATIONAL UNION OF CRYSTALLOGRAPHY** ☐ is enclosed ☐ will follow

Purchase order No.

☐ Please invoice me

☐ I wish to pay by credit card

EU authors only: VAT No:

Date

Signature

DIGITAL PRINTED REPRINTS

An electronic reprint is supplied free of charge.

Printed reprints without limit of number may be purchased at the prices given in the table below. The requirements of all joint authors, if any, and of their laboratories should be included in a single order, specifically ordered on the form overleaf. All orders for reprints must be submitted promptly.

Prices for reprints are given below in **United States dollars** and include postage.

Number of reprints required	Size of paper (in printed pages)				
	1–2	3–4	5–8	9–16	Additional 8's
50	184	268	372	560	246
100	278	402	556	842	370
150	368	534	740	1122	490
200	456	664	920	1400	610
Additional 50's	86	128	178	276	116

PAYMENT AND ORDERING

Official purchase orders should be made out to **INTERNATIONAL UNION OF CRYSTALLOGRAPHY**.

Orders should be returned by email to checkin@iucr.org

ENQUIRIES

Enquiries concerning reprints should be sent to support@iucr.org.